Ultrafast Zero-bias Surface Photocurrent in Germanium Selenide: Promise for Terahertz Devices and Photovoltaics

Kateryna Kushnir[1], Ying Qin[2], Yuxia Shen[2], Guangjiang Li[1], Benjamin M. Fregoso[3], Sefaattin Tongay[2] and Lyubov V. Titova[1*]

[1] Department of Physics, Worcester Polytechnic Institute, Worcester, Massachusetts 01609, USA

[2] School for Engineering of Matter, Transport and Energy, Arizona State University, Tampe, AZ 85287, USA

[3]Department of Physics, Kent State University, Kent, Ohio 44242, USA

**ltitova@wpi.edu*

Abstract:

Theory predicts that a large spontaneous electric polarization and concomitant inversion symmetry breaking in GeSe monolayers results in a strong shift current in response to their excitation in the visible range. Shift current is a coherent displacement of electron density on the order of a lattice constant upon above bandgap photoexcitation. A second order nonlinear effect, it is forbidden by the inversion symmetry in the bulk GeSe crystals. Here, we use terahertz (THz) emission spectroscopy to demonstrate that ultrafast photoexcitation with wavelengths straddling both edges of the visible spectrum, 400 nm and 800 nm, launches a shift current in the surface layer of a bulk GeSe crystal where the inversion symmetry is broken. The direction of the surface shift current determined from the observed polarity of the emitted THz pulses depends only on the orientation of the sample and not on the linear polarization direction of the excitation. Strong absorption by the low frequency infrared active phonons in the bulk of GeSe limits the bandwidth and the amplitude of the emitted THz pulses. We predict that reducing GeSe thickness to a monolayer or a few layers will result in a highly efficient broadband THz emission. Experimental demonstration of THz emission by the surface shift current in bulk GeSe crystals puts this 2D material forward as a candidate for next generation shift current photovoltaics, nonlinear photonic devices and THz sources.

Introduction

Theoretical investigations of group-IV monochalcogenides indicate that monolayer GeS, GeSe, SnS and SnSe exhibit a combination of extraordinary properties: high carrier mobility, strongly anisotropic electronic and optical properties that can be engineered by strain and controlled by external fields, and robust room temperature ferroelectricity.[1-4] A large spontaneous ferroelectric polarization of ~ 260-340 pC/m and the associated inversion symmetry breaking in monolayer GeSe is predicted to lead to extraordinarily large second-order electric susceptibilities responsible for nonlinear optical effects such as optical second harmonic generation, optical rectification and shift current.[4-8] A shift current is a zero-bias photocurrent resulting from a coherent spatial shift of the electron charge density in response to the excitation of an electron from the valence to the conduction band. [2-3, 5-6, 9-12] Pronounced nonlinear optical effects in the visible range that can be tuned by strain and external fields make monolayer GeSe and other

group-IV monochalcodenides a promising platform for a variety of applications in lasers, electro-optic modulators, switches, and frequency conversion devices.[13] In particular, an efficient optical rectification and/or shift current response can give rise to emission of terahertz (THz) radiation in response to excitation with laser pulses of sub-picosecond duration, putting GeSe forth as a candidate for THz sources for spectroscopy, imaging and high-speed communication.[14-15] Furthermore, the shift current is a mechanism behind the bulk photovoltaic effect (BPVE).[3, 6, 12, 16] BPVE-based GeSe solar cells may therefore provide an efficient alternative to traditional p-n junction-based ones [16-17].

While solution chemistry approaches and laser-assisted thinning show rapid progress towards the ultimate goal of reliable fabrication of large area, single crystalline GeSe monolayers, no experimental studies of nonlinear optical properties of GeSe monolayers have been reported to date.[18-19] On the other hand, GeSe single crystals with dimensions in millimeter range and larger can be reliably fabricated. Here, we present the first evidence of emission of THz pulses in response to above band gap photoexcitation of a bulk GeSe crystal with thickness approximately 100-200 μm and lateral dimensions of ~ 2 mm. We attribute THz generation to the shift current response in the surface layer of GeSe. While the stacking sequence of the layers in this van der Waals material yields a centrosymmetric bulk structure that corresponds to the D_{2h} (mmm) point group (Figure 1a), inversion symmetry is broken at the surface, and a spontaneous surface polarization can exist in the armchair direction just as it does in a monolayer GeSe. [7, 9] Efficient THz generation has been previously reported in arrays of sub- μm thick nanosheets of another group IV monochalcogenide, GeS, and at that time was attributed either to a surface shift current or to emission from a small number of nanosheets with the low, odd number of layers with broken inversion symmetry.[3, 20] Unlike the disordered array of GeS nanosheets, the present work focused on a macroscopic GeSe crystal, conclusively showing that THz generation in bulk-like group-IV monochalcogenides is a surface effect. Excitation fluence, orientation and excitation polarization dependence of the THz emission confirm that shift currents flow along one crystallographic direction, presumably determined by the spontaneous polarization of the surface layer. Stronger THz emission in response to 400 nm excitation than to the comparable fluence of 800 nm excitation stems from stronger absorption of 400 nm light by GeSe which leads to the higher excitation of a surface layer.[21] Highly efficient shift current photoexcitation in GeSe and the optical absorption that covers the entire visible range suggest applications of these layered materials in third generation BPVE photovoltaics and nonlinear photonic devices. Finally, surface selectivity of THz emission may lead to new approaches to chemical sensing.

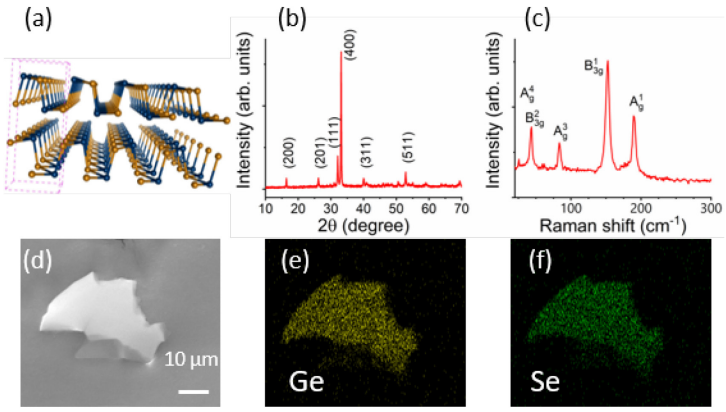

Figure 1. (a) Structural model of GeSe crystal. Structural characterization: powder x-ray diffraction (b) and bulk Raman spectroscopy (c) showing orthorhombic crystal structure of GeSe crystal. (d) Scanning electron microscopy image of a small GeSe flake mechanically exfoliated from the same bulk GeSe crystal that the one used in THz measurements, and the corresponding energy dispersive x-ray spectroscopy maps showing uniform distribution of Ge (e) and Se (f).

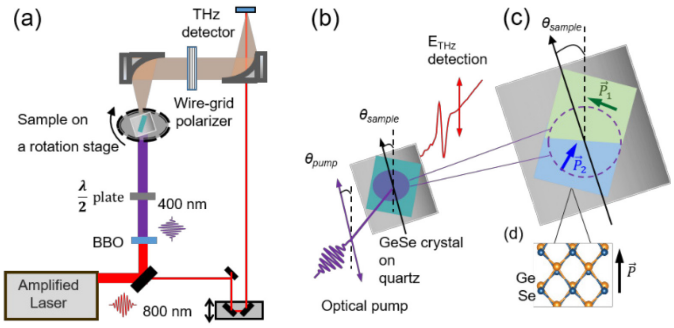

Figure 2. (a) Schematic diagram of the THz emission spectroscopy experiment. (b) Illustration of the experimental geometry where sample orientation and linear polarization of an optical pump pulse are varied relative to the fixed polarization of the detected THz pulses. (c) Schematic depiction of a GeSe crystal consisting of two crystal grain, each characterized by a spontaneous electric polarization vector along the armchair direction in the surface layer of GeSe[5-6] (d).

Results and discussion

We have used THz emission spectroscopy to study ultrafast dynamics of photoexcitation in a bulk GeSe crystal grown by chemical vapor transport technique. For measurements, a ~ 100-200 µm thick crystal of ~ 2 mm lateral dimensions was exfoliated from as-grown bulk crystal using adhesive tape. In addition, other small exfoliated pieces from the same crystal were used for structural characterization (Figure 1b-1f). THz emission spectroscopy allows electrical contact-free, all-optical monitoring of transient real or polarization photocurrents by detecting, in the far

field, THz radiation emitted by those currents.[11, 20, 22-27] We have performed THz emission measurements in transmission mode, with excitation and emission normal to the sample and therefore to the basal plane of GeSe crystal, as illustrated schematically in Figure 2. Sample orientation was varied by rotation of a sample stage through an angle θ_{sample}, and the polarization of the optical pump pulse (θ_{pump}) was varied by a half-wave plate. We find that photoexcited GeSe crystal emits nearly single-cycle THz pulses in response to either 800 nm (1.55 eV) or 400 nm (3.10 eV) excitation (Figure 3). With the linearly polarized excitation and detection at normal incidence (Figure 2) we can only detect THz emission due to the real or polarization currents parallel to the crystal surface, ruling out photo-Dember effect, photon drag, or emission due to drift of photoexcited carriers in built-in fields that are normal to the surface. In the absence of an external in-plane bias, possible mechanisms behind the observed THz emission involve second order nonlinear processes. A single color, linearly polarized excitation precludes injection current. As both excitation energies are larger than ~ 1.2 eV band gap, real free carriers are excited and the shift current, associated with the interband polarization, dominates over non-resonant optical rectification.[28-31] The observed THz emission thus indicates that above band gap excitation results in a shift current not only in GeSe monolayers, as has been predicted, but also in bulk GeSe crystals. Shift current resulting from excitation with ultrafast pulses gives rise to THz emission that varies as $\vec{E}_{shift} \propto \vec{J}_{shift}$ immediately above the GeSe surface, and again, reimaged onto the ZnTe detector crystal with the help of the parabolic mirrors.[22, 25, 32]

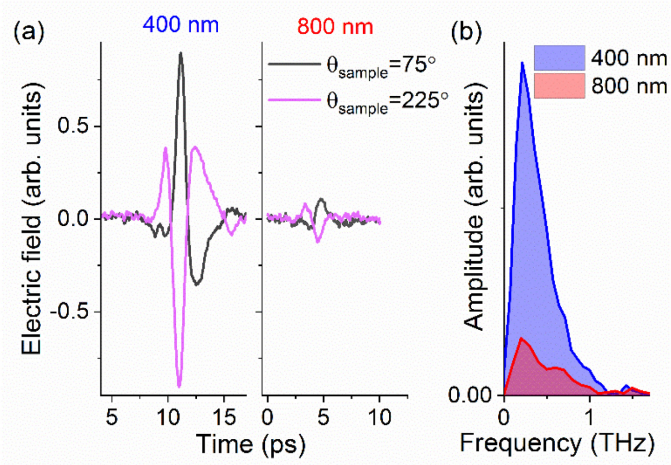

Figure 3. (a) THz waveforms emitted by the GeSe crystal as a result of excitation either with ~ 190 μJ/cm^2, 100 fs, 400 nm pulses (left panel) or with ~ 130 μJ/cm^2, 100 fs, 800 nm pulses (right panel), with θ_{pump} =0° in both cases. Rotating the crystal by 180° reverses polarity of the emitted pulse. (b) Amplitude spectra of the THz waveforms excited with 400 nm and 800 nm pulses taken with θ_{sample} =75°.

Ashift current is a second order nonlinear effect and thus requires a broken inversion symmetry. In GeSe *monolayers*, inversion symmetry is broken by a spontaneous lattice strain and puckering, which results in a polar point group C_{2v} (mm2) symmetry and a concurrent large (260-340 pC/m)

spontaneous polarization[4-7]. Inversion symmetry breaking is predicted to manifest in a pronounced zero-bias in-plane shift current upon above the band gap photoexcitation.[3, 5-8, 10] Unlike the monolayers, bulk GeSe is characterized by the centrosymmetric the D_{2h} (mmm) point group due to anti-ferroelectric stacking of consecutive layers (Figure 1a). However, inversion symmetry is broken at the surface, suggesting that the observed THz emission is due to a *surface* rather than *bulk shift current*.

Analysis of the differences of THz emission following 400 nm and 800 nm supports the surface origin of the observed THz emission. Assuming that the shift current in the top surface layer of a GeSe bulk crystal is qualitatively similar to that in a monolayer, shift current magnitude is expected to peak strongly immediately above the band gap and then fall off at higher energies.[5-6] As the optical penetration length of both 400 nm and 800 nm is significantly shorter than the thickness of the crystal[21], the bottom surface does not contribute. We find that the spectrally integrated amplitude of the THz waveforms emitted following excitation with 800 nm (1.55 eV) is nearly 20% of that for 400 nm excitation (3.10 eV) (Figure 3b). We find that the spectrally integrated amplitude of the THz waveforms emitted following excitation with 800 nm (1.55 eV) is nearly 20% of that for 400 nm excitation (3.10 eV) (Figure 3b). Taking into account a ~ 30% difference in excitation fluence, 400 nm pulses result in ~ 3.5 times stronger emission for equivalent incident excitation fluence. However, the absorption coefficient is ~ 10-fold higher at 400 nm compared to 800 nm (~0.078 nm-1 vs ~0.009 nm-1 at 800 nm)[21]. Taking into account reflection losses (~47% for 400 nm and ~41% for 800 nm)[21], and using 0.25 nm as the thickness of a GeSe monolayer[33], we calculate that equal incident excitation fluence results in ~ 7.7 times higher fluence or, equivalently, ~ 3.85 times higher number of photons absorbed in the top-most GeSe layer. Assuming that each absorbed photon promotes one electron from the valence to the conduction band, we find the contribution to the THz emission of each photon absorbed in the surface layer to be approximately equal regardless of its wavelength.

The amplitude of the observed THz emission peaks between 0.2 and 0.5 THz (Figure 3b). Temporal behavior of the shift current can be phenomenologically modeled as a convolution of the temporal derivative of the charge displacement with the pump intensity envelope.[22] For the pump pulse of ~ 100 fs duration, it is expected to vary on sub-picoseconds time scale with the bandwidth of the emitted THz radiation extending to ~ 10 THz.[20, 22] In the previous work on GeS nanosheets, we found that the bandwidth of the ZnTe detector crystal limited the observed bandwidth of THz emission.[20] However, in the case of GeSe, strong THz absorption by the sample itself is a limiting factor in uncovering the true ultrafast transient behavior of the surface shift currents from the THz pulses detected in the transmission geometry, as shown in Supporting Information (Figure S1). GeSe crystal absorbs over 80% of incident THz radiation that was generated in a 1 mm thick [110] ZnTe crystal, with absorbance increasing nearly five-fold between 0.2 to 1.8 THz. Strong THz absorption can be attributed to low frequency B_{3u} and B_{1u} infrared active phonons centered in the 2.5-2.6 THz range. B_{3u} phonons in particular are associated with opposite motion of Ge and Se along the armchair direction and couple strongly to the THz radiation polarized along this direction. As a result, GeSe crystal itself acts as a low pass filter, attenuating THz pulses emitted by the surface layer and broadening them to 1-2 ps in duration, as shown in Supporting Information (Figure S2). Reducing the GeSe thickness to

minimize re-absorption of the emitted THz radiation would result in a broadband source with efficiency surpassing that of conventional sources, as illustrated in Figure S1.

Figure 3a also shows that rotating the sample by 180° while maintaining an unchanged pump polarization reverses the polarity of emission while the amplitude and temporal shape of the waveform show only minimal change. This observation unequivocally shows that the inversion symmetry breaking in the surface layer of GeSe dictates the emission polarity and supports the surface shift current as a mechanism of THz generation.

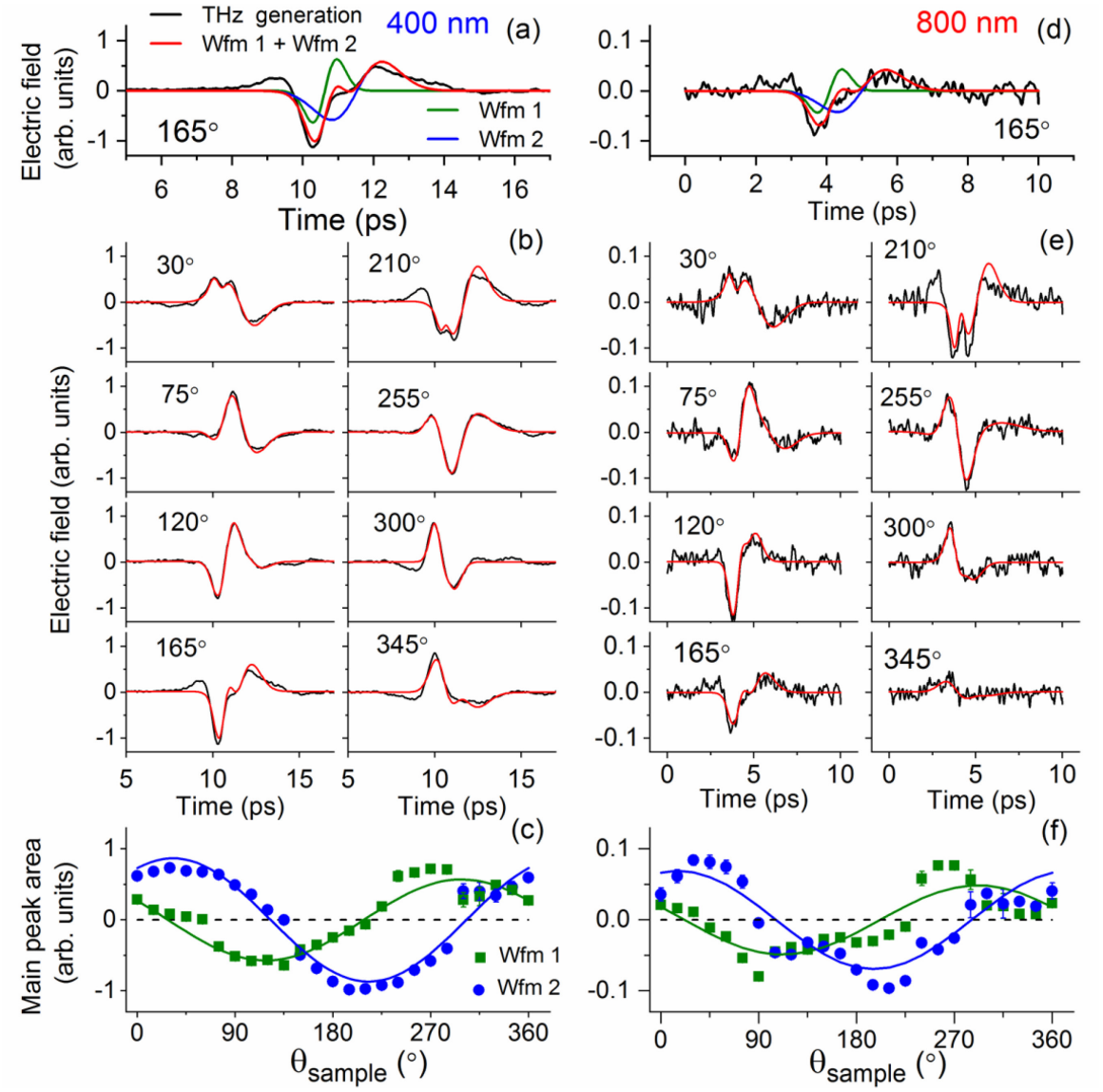

Figure 4. Dependence of THz emission excited with ~ 190 μJ/cm^2, 100 fs, 400 nm pulses (a-c) or with ~ 130 μJ/cm^2, 100 fs, 800 nm pulses (d-f), with θ_{pump} =0° in both cases. (a) and (d) show examples of decomposition of the observed emission in two single cycle transients, waveform 1 (Wfm 1) and waveform 2 (Wfm 2), corresponding to two crystal grains with different intrinsic surface polarizations in the excitation spot, as illustrated schematically in Figure 2c. (b) and (e) show emitted waveforms (black curves) and model fits to two transients (red curves) at different

sample orientations. (c) and (f) show area under the first peak of each of the two waveforms as a function of sample orientation. Symbols show the areas obtained from best model fits to the observed THz transients, and solid lines represent the fit of the data to a cosine function.

Figure 4 provides a detailed analysis of THz emission dependence on sample orientation. While the amplitude of the THz emission is nearly an order of magnitude lower for 800 nm excitation, the waveforms for the two excitation wavelengths are qualitatively the same for every sample orientation. As Figures 4a and 4d demonstrate, the observed waveform shape for both 400 nm and 800 nm excitation is well-described by a sum of two simple single-cycle bipolar Gaussian waveforms (e.g., the first derivatives of the Gaussian pulses, Figure S3). This decomposition of THz emission into two single cycle transients at all sample orientations suggests the presence of two crystal grains within a 1.5 mm photoexcited area on the GeSe crystal, each characterized by a specific spontaneous polarization vector ***P*** that dictates the direction of the surface shift current. Figure 2c schematically illustrates the two grain as side-by-side as a result of a stacking fault; however, it is also possible that they fully or partially overlap, or that they originate from a rotational misalignment between GeSe layers within a crystal. Each of the two transients is bipolar, indicating that momentum relaxation time is shorter that the pump pulse duration and does not affect the emitted waveform shape in a significant way.[20, 22] One of the single cycle waveforms (labeled as Wfm 1) has a Gaussian full width at half maximum (FWHM) of 1.0 ps ±0.3 ps. Another one (Wfm 2) is delayed by 1.1 ps ±0.2 ps and has a FWHM of 1.9 ps ±0.6 ps. Delay in arrival time and longer duration of the second waveform indicate that the thickness of the crystal grain that emits Wfm2 is larger. Figures 4b and 4c show model fits to experimental THz waveforms excited by 400 nm and 800 nm pulses. While simple Gaussian derivative pulses cannot account for a possible spectral chirp in each of the constituent pulses after propagation through the crystal, they adequately capture sample orientation dependence of emitted THz waveforms. Figures 4c and 4f plot the area under each of the model single cycle bipolar waveforms, with a sign that accounts for the polarity of the first peak of each waveform. For both waveforms, signed area follows a cosine dependence on the sample orientation. As we detect only one linearly polarized component of the emitted transient electric field, cosine dependence on sample orientation confirms that the shift current direction is determined by the intrinsic spontaneous surface polarization and associated inversion symmetry breaking of each crystalline grain. Shift current flows along the spontaneous polarization and emits electromagnetic radiation with electric field along this direction. Experimental waveforms represent a component of the emitted electromagnetic transient polarized along the detection axis. We find that for both 400 nm and 800 nm, waveform 1 has a positive maximum when the sample is rotated by 68° ± 4°from the (arbitrarily chosen) origin, while waveform 2 peaks at -30° ± 4°, with ~ 98° between the polarization directions in the two grains. Those angles indicate the direction of the photoexcited shift current in each of the grains.

The direction of the shift current, given by the spontaneous surface electric polarization, is presumed to be in a softer, armchair direction of GeSe lattice. We also expect strong THz

absorption due to the infrared active low frequency polar phonons to exhibit a significant dependence on the crystal orientation relative to the polarization of the incident THz radiation. B_{3u} phonon in particular involves motion of Ge and Se atoms in opposite directions along the armchair crystal direction and can therefore couple strongly to the THz radiation polarized along this direction. Indeed, such dependence exists. As shown in Figure 5, incident THz pulse from a ZnTe source is not only strongly attenuated but also split into two pulses delayed by ~ 1.1 ps due to transmission through the two, a thinner and a thicker, grains in the 1.5 mm diameter THz spot size on the studied GeSe crystal (Fig. 5(a)). Attenuation of the pulse transmitted through each grain is the strongest when it is polarized along the same direction as the THz pulses emitted by GeSe surface layer. For θ_{sample} of 150° or 330°, spontaneous electric polarization of the thicker grain ($\boldsymbol{P_2}$) is approximately parallel to the incident THz polarization, and the second (delayed) peak is not present. At the same time, the polarization of the thinner grain has a large component that is perpendicular to the incident THz polarization, resulting in an incomplete attenuation of the first peak. We observe the opposite trends for sample orientations of 90° and 270° where the first peak is almost fully attenuated while a small fraction of the second peak remains after propagation through the crystal. These results confirm that polarization of the THz pulses emitted by the surface shift current in GeSe coincides with the direction of strongest attenuation by the infrared active phonons, underscoring that thinner crystals will result in a much brighter THz source.

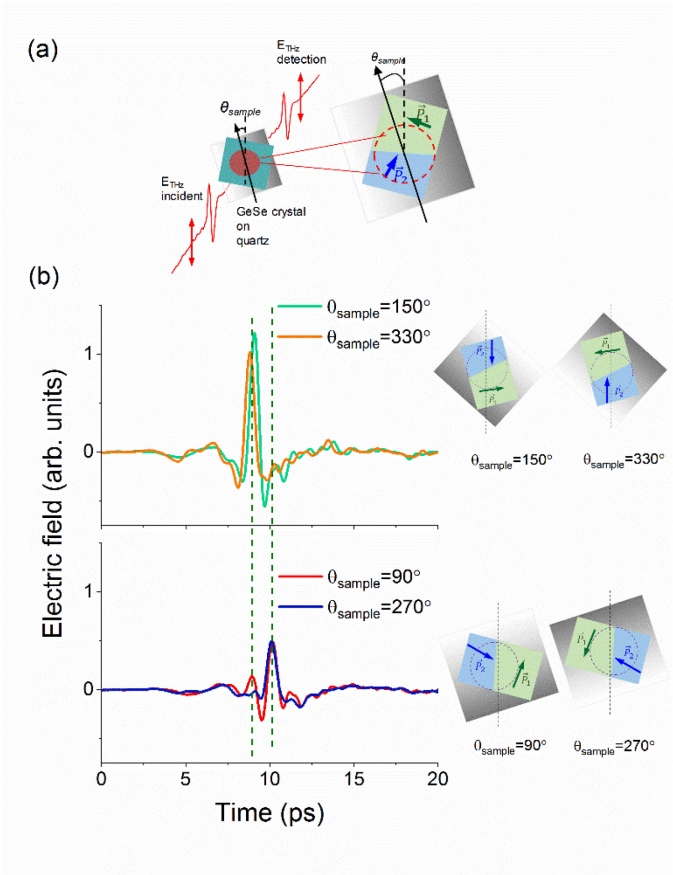

Figure 5. (a) Schematic diagram of measurement of absorption of incident THz pulses generated in a ZnTe source by GeSe crystal as a function of GeSe orientation. (b) Transmission of a THz pulse through two grains with different thickness and orientations splits the incident pulse into two. When polarization of the incident THz pulse has a large component parallel to the spontaneous electric polarization in a grain, its absorption is significantly stronger.

We also find that the amplitude, shape and polarity emitted THz waveforms are insensitive to the linear polarization of the pump pulse (Figure 6). Amplitude of the shift current can be expressed as:

$$J_a = \frac{c\varepsilon_0}{2}\kappa^{abb}E_b(\omega)E_b(-\omega), \quad (1)$$

where J_a is current in the *a* direction, $E_b(\omega)$ is electric field of the optical excitation at frequency ω polarized in the *b* direction, κ^{abb} is a photoresponsivity tensor, c is the speed of light, and ε_0 is the permittivity of free space.[34] In GeSe, like in other ferroelectric group-IV monochalcogenides, shift current flows in the direction of polarization, and J_a=J_x, where *x* is the armchair direction.[6] Given a significant structural anisotropy of the crystal lattice structure between the armchair and zigzag direction, the observed independence of the shift current on pump polarization is unexpected. DFT calculation of κ^{xxx} and κ^{xyy} for a GeSe monolayer demonstrates that while both functions have complicated and different energy dependence, there are multiple points along the energy axis where they cross, yielding a shift current that is independent on pump polarization. Our data shows that this is the case for 400 nm (3.1 eV) excitation, and $\kappa^{xxx} = \kappa^{xyy}$ at this energy.

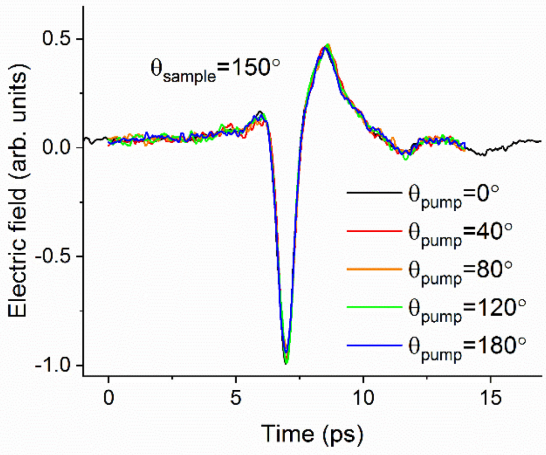

Figure 6. Selected THz waveforms excited by ~ 190 μJ/cm^2, 400 nm pulses with different pump linear polarization directions.

Finally, as expression (1) shows, we expect shift current to depend linearly on excitation fluence. We find that increasing 400 nm excitation fluence increases the amplitude of the emitted THz waveforms but does not change the shape of the waveforms (Figure 7(a)) or the bandwidth of the emitted radiation (Figure 7b). The inset to Figure 7b shows that the spectrally integrated electric field of THz pulses emitted by the GeSe crystal, which includes contributions of both crystalline grains present in the 1.5 mm diameter photoexcited area, and therefore the transient shift current varies linearly in response to the excitation fluence.

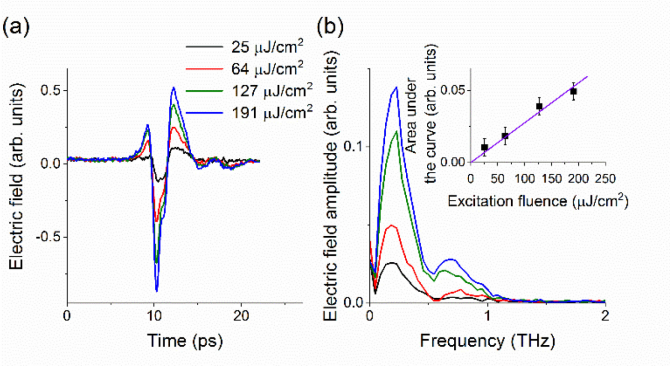

Figure 7. Excitation fluence dependence of THz generation in GeSe. (a) THz waveforms at different 400 nm photoexcitation fluence values. (b) The corresponding electric field spectral amplitude. Measurements were carried out with θ_{pump} =0° and θ_{sample} =180°.

In conclusion, we have presented the evidence of a surface shift current response in a bulk GeSe crystal. While the stacking sequence of the layers in this van der Waals material results in the inversion symmetry in the bulk, this symmetry is broken at the surface. We find that photoexcited GeSe crystals emit nearly single-cycle THz pulses in response to either 800 nm (1.55 eV) or 400 nm (3.10 eV) excitation. Excitation fluence, sample orientation and excitation polarization dependence of the THz emission confirm that shift current flowing along the spontaneous polarization of the surface layer is responsible for the observed emission. Stronger THz emission in response to 400 nm excitation compared to the comparable fluence of 800 nm excitation stems from stronger absorption of 400 nm light by GeSe which leads to the higher excitation of a surface layer. Highly efficient shift current in response to photoexcitation on the both short- and long-wave edges of the visible spectrum suggest applications of these layered materials in solar cells based on the bulk photovoltaic effect. BPVE photovoltaics. Efficient THz emission that is potentially tunable by strain can also be harnessed in the new nonlinear photonic devices, sensors and THz sources.

Experimental Section.

GeSe fabrication. GeSe single crystals were synthesized using chemical vapor transport growth technique using Ge (99.9999% purity), Se (99.9999% purity) pieces. These precursors were mixed at atomic 50:50% ratios and sealed into 0.5 inches diameter and 9 inches long quartz tubes under 10^{-6} Torr pressure. Extra GeI_4 powder was added as a transport agent to initiate the crystal growth

and successfully transport Ge, Se atomic species. Closely following Ge-Se binary phase diagrams, we have set the growth temperature at 550°C and cold temperature zone at 500°C for 5 weeks to complete the growth. Samples were cooled down to room temperature and ampoules were opened in a chemical glove box. Samples were characterized using x-ray diffraction (XRD, Figure 1b), Raman spectroscopy (Figure 1c), scanning electron microscopy (SEM, Figure 1d), and energy dispersive x-ray spectroscopy (EDS, Figures 1e and 1f).

THz emission spectroscopy. For THz emission spectroscopy measurements, a GeSe crystal with lateral dimensions of ~ 2 mm was excited at normal incidence with either 400 nm or 800 nm, 100 fs laser pulses from a 1 kHz amplified Ti:Sapphire source, as illustrated schematically in Figure 2. The sample was placed behind a 1.5 mm diameter aperture (not shown) in the center of ~ 7mm diameter collimated excitation beam to ensure uniformity of excitation. The thickness of the samples is estimated to be on the order of 100-200 μm. A 1 mm thick fused quartz slide was placed over the crystal to fix it on the sample stage. A pair of off-axis parabolic mirrors focused the emitted THz pulses from GeSe crystal within a 1.5 mm diameter photoexcited spot on a sample indicated by a circle in Figure 2 onto a [110] ZnTe crystal where they were coherently detected by free-space electro-optic sampling.[14] The wire-grid polarizer (Microtech Instruments; field extinction ratio of 0.01) ensured that only a component of the generated THz pulses polarized in the direction, labeled as E_{THz} detection direction in Figure 2b, was detected. Sample orientation was varied by rotation of a sample stage through an angle θ_{sample}, and the polarization of the optical pump pulse (given by the angle of pump polarization relative to vertical, θ_{pump}) was varied by a half-wave plate.

Acknowledgements

We acknowledge support from the NSF DMR-1750944 (LVT) and NSF DMR-1552220 (ST) and NERSC-DOE DE-AC02-05CH11231 (BMF).

Supporting Information Available:

Supporting Information

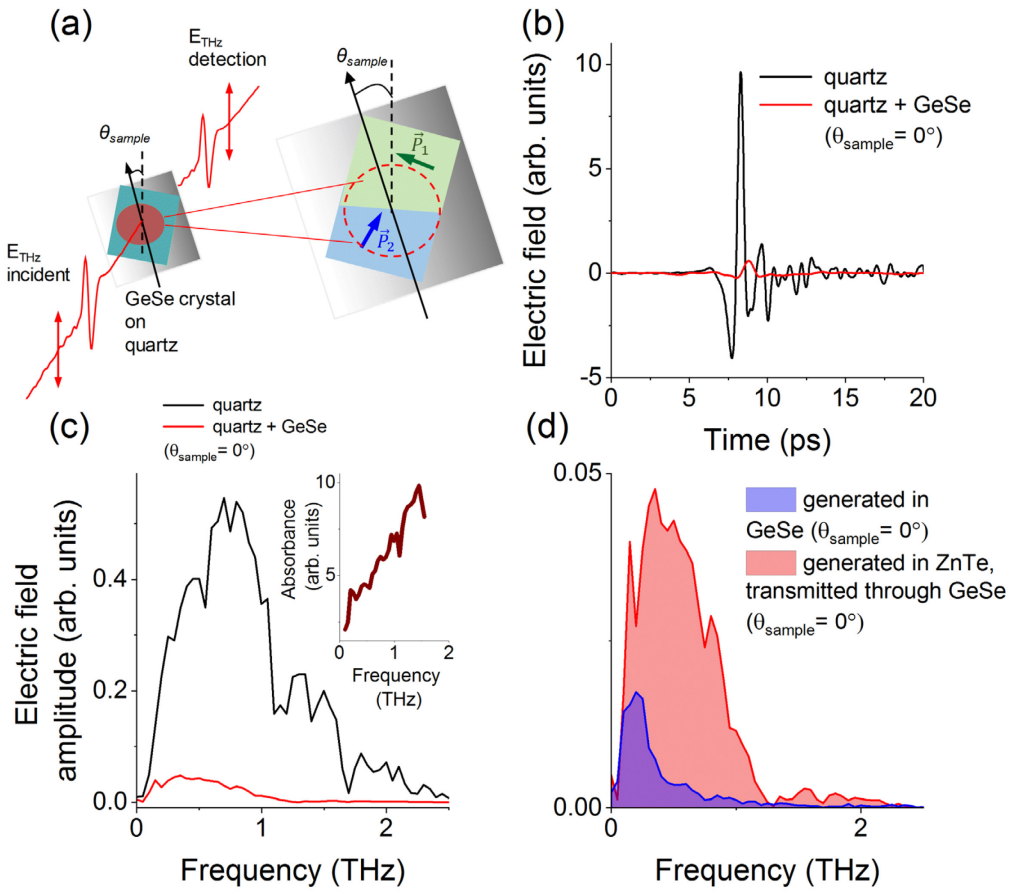

Supplementary Figure S2. (a) Illustration of the experimental geometry for measuring THz absorbance of a GeSe crystal: linear polarization of THz pulses generated by optical rectification of 800 nm, 100 fs pulses in a 1 mm thick [110] ZnTe crystal is parallel to the detection orientation. Orientation of the GeSe crystal is varied by the rotation of the sample stage. (b) Waveforms of the THz pulse generated in a 1 mm thick [110] ZnTe crystal and transmitted through a fused quartz slide used to hold the GeSe crystal in place on a sample stage, and through the GeSe crystal on the quartz slide. (c) Corresponding THz amplitude spectra. Inset shows THz absorbance of the GeSe crystal as a function of frequency. (d) Comparison of the amplitude spectra corresponding to THz emission from ZnTe optical rectification source in response to ~ 1000 μJ/cm^2, 800 nm pulses, and from the GeSe crystal in response to ~ 190 μJ/cm^2, 400 nm pulses.

Figure S1 (d) allows us to estimate efficiency of THz generation in GeSe by comparing it to THz generation in ZnTe, a THz source that is ubiquitous in THz spectroscopy applications. We find that the total emitted power as determined by the area under the amplitude curve, is 5.3 times higher for ZnTe. However, the fluence is ~ 5 times higher, and the total emitting area (~ 1 cm^2) is 15 times higher for ZnTe. Direct comparison is complicated by the fact that THz emission in GeSe is a surface effect and in the case of ZnTe it is a bulk effect with efficiency that scales linearly with the interaction length. With this caveat, per area and per incident fluence, efficiency of TH generation in GeSe per area and per incident fluence is over an order of magnitude higher. This estimate suggests that GeSe is very promising as a THz source, if large area, single crystalline monolayers can be isolated for this purpose.

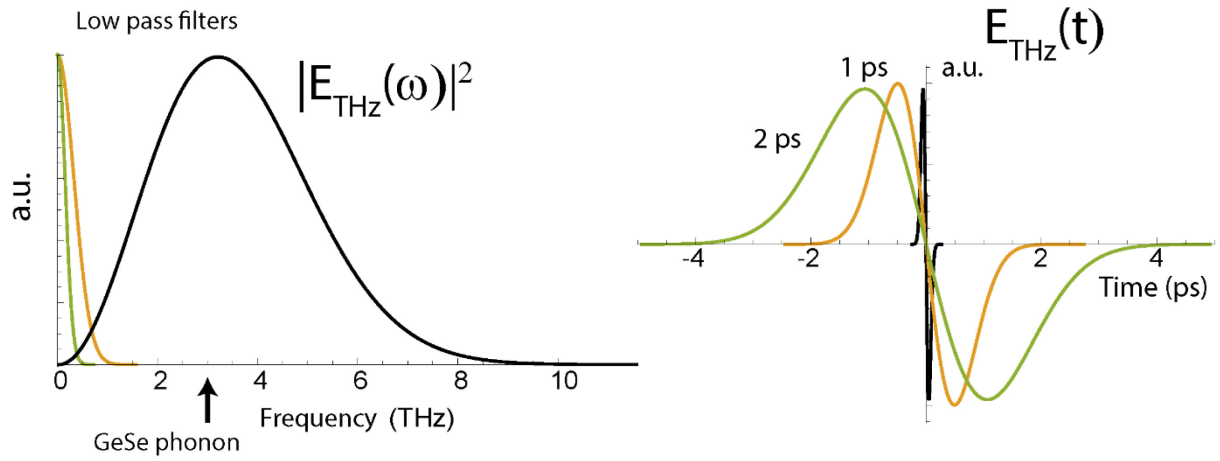

Supplementary Figure S2. (a) Illustration of the effect of GeSe B3u and other infrared-active phonons in ~ 2.5 THz spectral range on the bandwidth and temporal profile of the THz pulses emitted by the surface layer and transmitted through the crystal. Black curves show the power spectrum (left) and simulated waveform of the emitted THz pulse. Green and orange curves (left) simulate low pass filter-like influence of propagation through GeSe crystal, with the resulting waveforms shown in on the right. The precise width of the filter function and the resulting waveform depend on the crystal thickness.

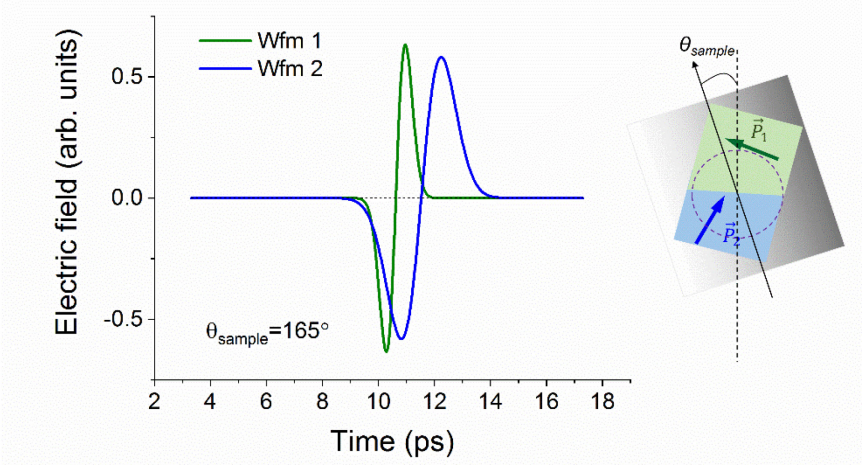

Supplementary Figure S3. Model single cycle waveforms (Gaussian pulse derivatives) used to represent THz waveforms emitted by the surface shift current and transmitted through a few μm thick GeSe crystal. Each of the two waveforms represents emission by a shift current in a single crystalline grain, with the current direction determined by a spontaneous surface electric polarization in a specific grain, as illustrated in a schematic on the right. Based on the experimental observations, studied GeSe crystal had two distinct grains in a 1.5 mm diameter field of view, one with the polarization ~ - 68° relative to the detection axis, and another one - ~30°.

References

(1) Wu, M. H.; Zeng, X. C. Intrinsic Ferroelasticity and/or Multiferroicity in Two-Dimensional Phosphorene and Phosphorene Analogues. *Nano Lett.* **2016,** *16* (5), 3236-3241, DOI: 10.1021/acs.nanolett.6b00726.
(2) Fei, R.; Kang, W.; Yang, L. Ferroelectricity and Phase Transitions in Monolayer Group-IV Monochalcogenides. *Phys. Rev. Lett.* **2016,** *117* (9), 097601.
(3) Cook, A. M.; B, M. F.; de Juan, F.; Coh, S.; Moore, J. E. Design principles for shift current photovoltaics. *Nat Commun* **2017,** *8*, 14176, DOI: 10.1038/ncomms14176.
(4) Hua Wang and Xiaofeng, Q. Two-dimensional multiferroics in monolayer group IV monochalcogenides. *2D Materials* **2017,** *4* (1), 015042.
(5) Panday, S. R.; Fregoso, B. M. Strong second harmonic generation in two-dimensional ferroelectric IV-monochalcogenides. *Journal of Physics-Condensed Matter* **2017,** *29* (43), DOI: 10.1088/1361-648X/aa8bfc.
(6) Rangel, T.; Fregoso, B. M.; Mendoza, B. S.; Morimoto, T.; Moore, J. E.; Neaton, J. B. Large Bulk Photovoltaic Effect and Spontaneous Polarization of Single-Layer Monochalcogenides. *Phys. Rev. Lett.* **2017,** *119* (6), 067402, DOI: 10.1103/PhysRevLett.119.067402.
(7) Wang, H.; Qian, X. Giant Optical Second Harmonic Generation in Two-Dimensional Multiferroics. *Nano Lett.* **2017,** *17* (8), 5027-5034, DOI: 10.1021/acs.nanolett.7b02268.
(8) Fregoso, B. M.; Morimoto, T.; Moore, J. E. Quantitative relationship between polarization differences and the zone-averaged shift photocurrent. *Physical Review B* **2017,** *96* (7), 075421, DOI: 10.1103/PhysRevB.96.075421.
(9) Fei, R.; Li, W.; Li, J.; Yang, L. Giant piezoelectricity of monolayer group IV monochalcogenides: SnSe, SnS, GeSe, and GeS. *Appl. Phys. Lett.* **2015,** *107* (17), 173104, DOI: doi:http://dx.doi.org/10.1063/1.4934750.
(10) Mehboudi, M.; Fregoso, B. M.; Yang, Y.; Zhu, W.; van der Zande, A.; Ferrer, J.; Bellaiche, L.; Kumar, P.; Barraza-Lopez, S. Structural Phase Transition and Material Properties of Few-Layer Monochalcogenides. *Phys. Rev. Lett.* **2016,** *117* (24), 246802, DOI: 10.1103/PhysRevLett.117.246802.
(11) Schleicher, J. M.; Harrel, S. M.; Schmuttenmaer, C. A. Effect of spin-polarized electrons on terahertz emission from photoexcited GaAs. *J. Appl. Phys.* **2009,** *105* (11), 113116, DOI: doi:http://dx.doi.org/10.1063/1.3133093.
(12) Ogawa, N.; Sotome, M.; Kaneko, Y.; Ogino, M.; Tokura, Y. Shift current in the ferroelectric semiconductor SbSI. *Physical Review B* **2017,** *96* (24), 241203, DOI: 10.1103/PhysRevB.96.241203.
(13) Guan, S.; Liu, C.; Lu, Y.; Yao, Y.; Yang, S. A. Tunable ferroelectricity and anisotropic electric transport in monolayer β-GeSe. *Physical Review B* **2018,** *97* (14), 144104, DOI: 10.1103/PhysRevB.97.144104.
(14) Jepsen, P. U.; Cooke, D. G.; Koch, M. Terahertz spectroscopy and imaging–Modern techniques and applications. *Laser & Photonics Reviews* **2011,** *5* (1), 124-166.
(15) Tonouchi, M. Cutting-edge terahertz technology. *Nature photonics* **2007,** *1* (2), 97-105.
(16) Butler, K. T.; Frost, J. M.; Walsh, A. Ferroelectric materials for solar energy conversion: photoferroics revisited. *Energy & Environmental Science* **2015,** *8* (3), 838-848, DOI: 10.1039/C4EE03523B.
(17) Tan, L. Z.; Zheng, F.; Young, S. M.; Wang, F.; Liu, S.; Rappe, A. M. Shift current bulk photovoltaic effect in polar materials—hybrid and oxide perovskites and beyond. *Npj Computational Materials* **2016,** *2*, 16026, DOI: 10.1038/npjcompumats.2016.26.
(18) Zhao, H.; Mao, Y.; Mao, X.; Shi, X.; Xu, C.; Wang, C.; Zhang, S.; Zhou, D. Band Structure and Photoelectric Characterization of GeSe Monolayers. *Adv. Funct. Mater.* **2018,** *28* (6), 1704855, DOI: doi:10.1002/adfm.201704855.
(19) Ramasamy, P.; Kwak, D.; Lim, D.-H.; Ra, H.-S.; Lee, J.-S. Solution synthesis of GeS and GeSe nanosheets for high-sensitivity photodetectors. *J. Mater. Chem. C* **2016,** *4* (3), 479-485, DOI: 10.1039/c5tc03667d.

(20) Kushnir, K.; Wang, M.; Fitzgerald, P. D.; Koski, K. J.; Titova, L. V. Ultrafast Zero-Bias Photocurrent in GeS Nanosheets: Promise for Photovoltaics. *ACS Energy Letters* **2017**, 1429-1434, DOI: 10.1021/acsenergylett.7b00330.
(21) Liu, S.-C.; Mi, Y.; Xue, D.-J.; Chen, Y.-X.; He, C.; Liu, X.; Hu, J.-S.; Wan, L.-J. Investigation of Physical and Electronic Properties of GeSe for Photovoltaic Applications. *Advanced Electronic Materials* **2017,** *3* (11), 1700141, DOI: doi:10.1002/aelm.201700141.
(22) Braun, L.; Mussler, G.; Hruban, A.; Konczykowski, M.; Schumann, T.; Wolf, M.; Münzenberg, M.; Perfetti, L.; Kampfrath, T. Ultrafast photocurrents at the surface of the three-dimensional topological insulator Bi_2Se_3. *Nature Communications* **2016,** *7*, 13259, DOI: 10.1038/ncomms13259

http://www.nature.com/articles/ncomms13259#supplementary-information.
(23) Bieler, M.; Pierz, K.; Siegner, U.; Dawson, P. Shift currents from symmetry reduction and Coulomb effects in (110)-orientated GaAs\$Al_{0.3}Ga_{0.7}$As quantum wells. *Physical Review B* **2007,** *76* (16), 161304.
(24) Laman, N.; Bieler, M.; van Driel, H. M. Ultrafast shift and injection currents observed in wurtzite semiconductors via emitted terahertz radiation. *J. Appl. Phys.* **2005,** *98* (10), 103507, DOI: doi:http://dx.doi.org/10.1063/1.2131191.
(25) Priyadarshi, S.; Leidinger, M.; Pierz, K.; Racu, A. M.; Siegner, U.; Bieler, M.; Dawson, P. Terahertz spectroscopy of shift currents resulting from asymmetric (110)-oriented GaAs/AlGaAs quantum wells. *Appl. Phys. Lett.* **2009,** *95* (15), 151110, DOI: 10.1063/1.3249611.
(26) Titova, L. V.; Pint, C. L.; Zhang, Q.; Hauge, R. H.; Kono, J.; Hegmann, F. A. Generation of Terahertz Radiation by Optical Excitation of Aligned Carbon Nanotubes. *Nano Lett.* **2015,** *15* (5), 3267-3272, DOI: 10.1021/acs.nanolett.5b00494.
(27) Bagsican, F. R.; Zhang, X.; Ma, L.; Wang, M.; Murakami, H.; Vajtai, R.; Ajayan, P. M.; Kono, J.; Tonouchi, M.; Kawayama, I. Effect of Oxygen Adsorbates on Terahertz Emission Properties of Various Semiconductor Surfaces Covered with Graphene. *Journal of Infrared, Millimeter, and Terahertz Waves* **2016,** *37* (11), 1117-1123, DOI: 10.1007/s10762-016-0301-x.
(28) Nastos, F.; Sipe, J. E. Optical rectification and shift currents in GaAs and GaP response: Below and above the band gap. *Physical Review B* **2006,** *74* (3), 035201, DOI: 10.1103/PhysRevB.74.035201.
(29) Côté, D.; Laman, N.; Driel, H. M. v. Rectification and shift currents in GaAs. *Appl. Phys. Lett.* **2002,** *80* (6), 905-907, DOI: 10.1063/1.1436530.
(30) Bieler, M. THz Generation From Resonant Excitation of Semiconductor Nanostructures: Investigation of Second-Order Nonlinear Optical Effects. *IEEE Journal of Selected Topics in Quantum Electronics* **2008,** *14* (2), 458-469, DOI: 10.1109/jstqe.2007.910559.
(31) Sipe, J. E.; Shkrebtii, A. I. Second-order optical response in semiconductors. *Physical Review B* **2000,** *61* (8), 5337-5352, DOI: 10.1103/PhysRevB.61.5337.
(32) Côté, D.; Sipe, J. E.; van Driel, H. M. Simple method for calculating the propagation of terahertz radiation in experimental geometries. *Journal of the Optical Society of America B* **2003,** *20* (6), 1374-1385, DOI: 10.1364/JOSAB.20.001374.
(33) Mounet, N.; Gibertini, M.; Schwaller, P.; Campi, D.; Merkys, A.; Marrazzo, A.; Sohier, T.; Castelli, I. E.; Cepellotti, A.; Pizzi, G.; Marzari, N. Two-dimensional materials from high-throughput computational exfoliation of experimentally known compounds. *Nature Nanotechnology* **2018,** *13* (3), 246-252, DOI: 10.1038/s41565-017-0035-5.
(34) Young, S. M.; Rappe, A. M. First Principles Calculation of the Shift Current Photovoltaic Effect in Ferroelectrics. *Phys. Rev. Lett.* **2012,** *109* (11), 116601.